

# A track-before-detect labelled multi-Bernoulli particle filter with label switching

Ángel F. García-Fernández

**Abstract**—This paper presents a multitarget tracking particle filter (PF) for general track-before-detect measurement models. The PF is presented in the random finite set framework and uses a labelled multi-Bernoulli approximation. We also present a label switching improvement algorithm based on Markov chain Monte Carlo that is expected to increase filter performance if targets get in close proximity for a sufficiently long time. The PF is tested in two challenging numerical examples.

**Index Terms**—Particle filters, MCMC, random finite sets, multitarget tracking, Kullback-Leibler divergence

## I. INTRODUCTION

In surveillance applications it is important to accurately estimate the number of targets along with their states at each time step based on a sequence of measurements. A relevant difficulty in this multitarget tracking (MTT) problem is the fact that the number of targets is unknown and time varying. Yet, Bayesian inference on multiobject systems, such as MTT, can be done in a mathematically rigorous way using the random finite set (RFS) formulation [1]. Here, the multitarget state is a set that contains the single target states and all the available information about the targets is included in the posterior probability density function (PDF), i.e., the PDF of the state given all available measurements [2]. In most cases of interest, calculating the posterior PDF is intractable due to nonlinear/non-Gaussian dynamic and measurement models and the difficulty of handling target births and deaths. Consequently, it must be approximated.

If a unique identifying label is added to each single target state, we can estimate the states of specific targets at different time steps [3], [4]. Moreover, the resulting Bayesian recursion is more easily performed because of the simplification of the set integrals in the prediction step [3], [5]. This implies that it can be useful to include target labels, which could be considered as auxiliary variables, even if we are only interested in performing inference on the unlabelled collection of targets. Importantly in this case, we have an extra degree of freedom that can be used to improve the posterior PDF approximation: we can choose any labelled posterior PDF as long as the corresponding unlabelled posterior PDF remains unaltered.

This kind of idea, which we refer to as label switching improvement, was first introduced for fixed and known number of targets and Gaussian approximations in [6]. It can lead to benefits in performance if there is mixed labelling [7], i.e., when targets get in close proximity for a sufficiently long time and then separate. An extension of [6] for MTT, with Gaussian multi-Bernoulli PDFs, has been proposed in [8].

In this paper, we first design an efficient particle filter (PF) [9] for track-before-detect MTT with no assumptions in the measurement model. Then, we develop an algorithm for label switching improvement for this PF based on Markov chain Monte Carlo (MCMC) [10]. We proceed to review the literature and explain our contributions more thoroughly.

As we focus on general track-before-detect applications, MTT algorithms for the radar point detection measurement model, such as the probability hypothesis density (PHD) filter [2], cardinalised PHD (CPHD) filter [11], multiple hypothesis tracking [12], the labelled RFS filters in [3], [13], [14] or the sequential Monte Carlo (SMC) algorithms in [15], [16] cannot be applied. There are multiple track-before-detect MTT algorithms that are not general as they require specific measurement models such as superpositional sensors [17], [18], models with likelihood factorisation over single targets [19], pixelised sensors [20]–[22] or the model of the histogram probabilistic multi-hypothesis tracker [23].

We address the track-before-detect problem for general measurement models by considering an approximation to the posterior PDF based on SMC methods or particle filters (PFs). Markov chain Monte Carlo (MCMC) methods can also be applied to perform Bayesian filtering with the same flexibility as PFs [24] but we focus on PFs. A PF provides an SMC approximation to the posterior which converges to the posterior as the number of particles tends to infinity under some conditions [25]. In practice however, it is desirable to keep the number of particles low to reduce the computational burden as well as increasing the speed of the filter. Due to the curse of dimensionality, direct generalisations of single target PFs to MTT do not work well for a reasonably low number of particles [4]. One way of alleviating this problem is to make the posterior independence assumption (PIA), in which target states are independent [4], [20], [26]–[28]. While PIA implies that the PF is no longer asymptotically optimal, it is usually beneficial for low sample sizes [27].

In order to account for the unknown and variable number of targets in PFs, one possibility is to sample target existences directly from the prior [29]. Yet, this is highly inefficient as it removes and adds targets regardless of the current measurement. In [20]–[22], the current measurement is taken

Copyright (c) 2016 IEEE. Personal use of this material is permitted. Permission from IEEE must be obtained for all other users, including reprinting/republishing this material for advertising or promotional purposes, creating new collective works for resale or redistribution to servers or lists, or reuse of any copyrighted components of this work in other works.

The author is with the Department of Electrical and Computer Engineering, Curtin University, Perth, WA 6102, Australia (email: angel.garciafernandez@curtin.edu.au).

This work was supported in part by the Australian Research Council under Discovery Project DP130104404.

into account to draw samples from target existences by an existence grid, and in [4], by a two-layer PF. However, in these cases, sampling of target existences and states is done via separate procedures, which can imply detrimental effects on performance if several targets are in close proximity. In this paper, we handle target states and label existences jointly using the labelled RFS framework by assuming a labelled multi-Bernoulli (LMB) posterior, which implies that target states and existences are independent [3]. The proposed PF, the generalised parallel partition (GPP) PF, is an extension of the parallel partition (PP) PF, which was developed for fixed and known number of targets [4, Sec. III]. In contrast to the PP method, the GPP method does not require a two-layer PF [4, Sec. IV] to take into account variable target number as the target states and existences are handled jointly. We generalise the PP method due to its computational efficiency and high performance [4], [27], [28].

As mentioned before, we can make use of label switching improvement techniques, which are useful if targets move in close proximity for a long time and we are not interested in labelling information [30]. In this respect, we propose an algorithm to obtain a PDF that does not alter the unlabelled target information and can be more accurately approximated as LMB than the original posterior PDF. This improvement in the LMB approximation enhances the performance of the particle filter. This algorithm is based on iterated Kullback-Leibler divergence (KLD) minimisations and is a generalisation of [31], which considers a fixed and known number of targets.

The remainder of the paper is organised as follows. We formulate the problem in Section II. Section III explains the recursion for improving the LMB approximation. In Section IV, we develop the GPP particle filter. The implementation of the label switching improvement algorithm for the particle filter is developed in Section V. Numerical examples are provided in Section VI. Finally, conclusions are drawn in Section VII.

## II. PROBLEM FORMULATION

In this paper, labelled RFS densities are denoted as  $\pi$ , unlabelled RFS densities as  $\tilde{\pi}$  and densities over a vector space as  $\pi$ , which are referred to as vector densities. A brief introduction to the RFS framework with unlabelled and labelled sets can be found in Sections II and III in [3]. Without loss of generality, we remove the time index of the filtering recursion for notational simplicity. Variables and densities at the previous time step have a superscript  $-$ .

The collection of targets at the current time step is represented by the unlabelled set  $X = \{x_1, \dots, x_t\}$ , where  $x_i \in \mathbb{R}^{n_x}$  is the state of the  $i$ th target. The multiobject transition density  $\tilde{f}(\cdot|X^-)$  encapsulates the underlying models of target dynamics, births and deaths. Targets are observed through noisy measurements, which can be vectors or sets. Once the measurement has been observed, the resulting multi-target likelihood  $\ell(\cdot)$  depends on  $X$  and with this notation we highlight that it is not a PDF on  $X$ . For the sake of notational simplicity, we omit the explicit value of the measurement in the likelihood.

The objective of this paper is to compute the unlabelled RFS posterior density  $\tilde{\pi}$ , whose argument is  $X$ , for general track-before-detect measurement models. The PDF  $\tilde{\pi}$  contains all information regarding the unlabelled states given the sequence of measurements. The filtering recursion is [1]

$$\tilde{\pi}(X) \propto \ell(X) \int \tilde{f}(X|X^-) \tilde{\pi}^-(X^-) \delta X^- \quad (1)$$

where  $\propto$  denotes proportionality.

Even though our objective is to calculate the unlabelled RFS posterior, using a labelled posterior is beneficial to perform the filtering recursion because set integrals are easier to compute [3], [5]. In this case, labels can be seen as auxiliary variables that aid in computation. We denote the labelled set as  $\mathbf{X} = \{(x_1, l_1), \dots, (x_t, l_t)\}$  where  $l_i \in \mathbb{L}$  is the label for the  $i$ th target, no two targets can have the same label and  $\mathbb{L}$  is a countable set. The filtering recursion becomes [1]

$$\pi(\mathbf{X}) \propto \ell(\mathbf{X}) \int \mathbf{f}(\mathbf{X}|\mathbf{X}^-) \pi^-(\mathbf{X}^-) \delta \mathbf{X}^- \quad (2)$$

where  $\pi$  is the labelled RFS posterior at the current time step and  $\mathbf{f}(\cdot|\mathbf{X}^-)$  is the labelled RFS transition density. It should be highlighted that  $\mathbf{f}(\cdot|\mathbf{X}^-)$  has the property that the labels of the surviving targets do not change with time. This is the main reason why the set integrals in (2) are easier to compute than in (1). Based on [6], we make the following definition.

**Definition 1.** The unlabelled RFS family  $[\pi]$  of  $\pi$  is  $[\pi] = \{\varphi : \varphi \sim \pi\}$ , where  $\varphi \sim \pi$  if and only if  $\varphi$  and  $\pi$  have the same unlabelled PDF, which is obtained by integrating out the labels [3, Eq. (9)]:

$$\begin{aligned} & \sum_{(l_1, \dots, l_t) \in \mathbb{L}^t} \varphi(\{(x_1, l_1), \dots, (x_t, l_t)\}) \\ &= \sum_{(l_1, \dots, l_t) \in \mathbb{L}^t} \pi(\{(x_1, l_1), \dots, (x_t, l_t)\}) \quad \forall t \in \mathbb{N}. \end{aligned}$$

Set  $[\pi]$  is an equivalence class as  $\sim$  is reflexive, symmetric and transitive. If the targets move independently with the same dynamics and measurements do not provide labelling information, we can calculate (1) using (2) by a labelled RFS density  $\pi^-$  such that if we integrate out the labels we obtain  $\tilde{\pi}^-$ . Importantly, at any time step, we can change the labelled RFS density  $\pi^-$  with another labelled density  $\varphi^- \in [\pi^-]$  at our convenience. These ideas were first used in [6] to provide more accurate Gaussian approximations in MTT with fixed and known number of targets.

In order to approximate the unlabelled posterior for general measurement models, this paper proposes a PF with LMB approximation. The prediction and update step are therefore performed via Monte Carlo sampling and the resulting PDF is approximated as LMB via KLD minimisation. Instead of performing the LMB approximation on the labelled posterior provided by the PF, we can choose another labelled PDF within its unlabelled RFS family that can be approximated as LMB more accurately to improve performance. This algorithm is designed based on KLD minimisations and implemented via MCMC. The resulting LMB-PF recursion is illustrated in Figure 1. The label switching improvement algorithm is explained

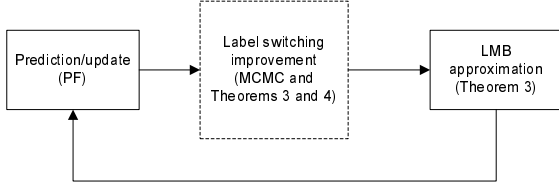


Figure 1: Diagram of the proposed LMB-PF recursion. The label switching improvement algorithm is optional as it is only useful if targets get in close proximity for a sufficiently long time and then separate.

in Section III, the PF in Section IV and the implementation of the label switching improvement for the PF based on MCMC in Section V.

### III. IMPROVEMENT OF LMB APPROXIMATION

In this section we describe the label switching improvement algorithm, see Figure 1. That is, given a labelled RFS density  $\pi$ , we provide a recursion of PDFs to select a labelled PDF that belongs to  $[\pi]$  that is more accurately approximated as LMB than  $\pi$ . First, we write a simplified expression for the KLD for labelled RFS in Section III-A. Second, we review LMB RFS in Section III-B. Third, we provide the required iterated optimisations in Section III-C. Fourth, in Section III-D, we provide an example to illustrate the results of this section.

#### A. Kullback-Leibler divergence

In this section, we derive a decomposition of the KLD for labelled sets. First, we introduce the required notation. Given a labelled RFS density  $\pi$  and  $t$  different labels  $l_1, \dots, l_t$ , we define the PDF (over a vector space) [5]

$$\pi(x_{1:t}; l_1, \dots, l_t) \triangleq \frac{\pi(\{(x_1, l_1), \dots, (x_t, l_t)\})}{P_\pi(\{l_1, \dots, l_t\})} \quad (3)$$

where

$$P_\pi(\{l_1, \dots, l_t\}) = \int \pi(\{(x_1, l_1), \dots, (x_t, l_t)\}) dx_{1:t} \quad (4)$$

is the probability of having a labelled set with labels  $\{l_1, \dots, l_t\}$  and  $x_{1:t} = (x_1, \dots, x_t)$ .

**Proposition 2.** *Given two labelled RFS densities  $\pi$  and  $\nu$ , the KLD [1]*

$$D(\pi \parallel \nu) = \int \pi(\mathbf{X}) \log \frac{\pi(\mathbf{X})}{\nu(\mathbf{X})} \delta \mathbf{X} \quad (5)$$

can be written as

$$D(\pi \parallel \nu) = D(P_\pi \parallel P_\nu) + \sum_{L \subseteq \mathbb{L}} P_\pi(L) D(\pi(\cdot; \vec{L}) \parallel \nu(\cdot; \vec{L})) \quad (6)$$

where  $\vec{L}$  is a vector whose components are the elements of  $L$  arranged in ascending order.

Proposition 2 is proved in Appendix A. We want to remark that Proposition 2 holds for any ordering  $\vec{L}$  of  $L$ . As pointed out in Section III-C, we use labels that are natural numbers, as in [4], [32], so we can use ascending order without loss of generality. If labels are vectors as in [3], we can define  $\vec{L}$  based on lexicographical order [33].

#### B. Labelled multi-Bernoulli RFS

An LMB density  $\nu$  is defined under the assumption

- A1 There is a maximum number  $\kappa$  of targets.

An LMB RFS includes a target with label  $j \in \mathbb{L}$  with probability  $p_j$  and, if this target exists, its state is distributed according to a density  $\nu(\cdot; j)$  independently from the rest of targets [3]. In this paper, we characterise its RFS density by

$$P_\nu(\{l_1, \dots, l_t\}) = \prod_{j=1}^{\kappa} (1 - p_j) \prod_{j=1}^t \frac{p_{l_j}}{1 - p_{l_j}} \quad (7)$$

$$\nu(x_{1:t}; l_{1:t}) = \nu(x_1; l_1) \dots \nu(x_t; l_t) \quad (8)$$

where we have assumed without loss of generality that  $\mathbb{L} = \{1, \dots, \kappa\}$ .

#### C. Iterated optimisations

In this section, ideally, we would like to find the best LMB approximation  $\nu$  to any density  $\varphi \in [\pi]$ . Therefore, given  $\pi$ , we would like to find

$$\nu^* = \arg \min_{\nu} D(\varphi \parallel \nu) \quad (9)$$

subject to  $\varphi \in [\pi]$  and  $\nu$  is LMB. However, this optimisation problem is difficult to solve.

Instead, in this paper, we provide a sequence of PDFs  $\varphi^0 = \pi$ ,  $\nu^0$ ,  $\varphi^1$ ,  $\nu^1, \dots$  such that at each step of the iteration the KLD is lowered. Specifically, based on  $\varphi^n$ ,  $\nu^n$  is obtained by minimising  $D(\varphi^n \parallel \nu^n)$  with constraints (7) and (8). How to perform this minimisation will be indicated by Theorem 3. Note that the result of this theorem provides us with the best LMB approximation to a labelled RFS density according to the KLD. Given  $\nu^n$ ,  $\varphi^{n+1}$  is calculated as follows. First, the algorithm sets  $P_{\varphi^{n+1}} = P_\pi$  so that the original probability mass function (PMF) of the labels does not change. Second, we set  $\varphi^{n+1}(\cdot; l_{1:t}) = \varphi^n(\cdot; l_{1:t})$  for all the labels  $\{l_1, \dots, l_t\} \subseteq \{1, \dots, \kappa\}$ . Then, we go through all the labels and modify  $\varphi^{n+1}(\cdot; l_{1:t})$  by minimising  $D(\varphi^{n+1} \parallel \nu^n)$  with constraint  $\varphi \in [\pi]$ . How to perform these minimisations will be indicated by Theorem 4. The resulting sequence is quite suitable for PF implementations, as will be seen in Section V. Due to how the minimisations are performed,

$$D(\varphi^n \parallel \nu^n) \geq D(\varphi^{n+1} \parallel \nu^n) \geq D(\varphi^{n+1} \parallel \nu^{n+1}). \quad (10)$$

This implies that the final LMB approximation is equal or more accurate than the original. As  $D(\varphi \parallel \nu) \geq 0$ , this sequence converges. The required optimisations are given below.

**Theorem 3.** *For a given labelled RFS density  $\varphi$ , the solution to*

$$\arg \min_{\nu} D(\varphi \parallel \nu)$$

subject to  $\nu$  being LMB, which implies (7) and (8), is

$$p_j = \sum_{L \ni j} P_\varphi(L) \quad (11)$$

$$\nu(x_1; j) \propto \sum_{L \ni j} P_\varphi(L) \varphi_j(x_1; \vec{L}) \quad j = \{1, \dots, \kappa\} \quad (12)$$

where  $\varphi_j(\cdot; \vec{L})$  denotes the marginal PDF of the state that corresponds to label  $j$  given the labels  $\vec{L}$ .

This theorem is proved in Appendix B. We want to remark that  $\varphi(\cdot; \vec{L})$  is a vector density so the marginal  $\varphi_j(\cdot; \vec{L})$  simply corresponds to integrating out the states except the one with label  $j$ . In [13, Sec. III.B], an LMB approximation from a  $\delta$ -generalised LMB PDF is proposed. Theorem 3 implies that the approximation provided in [13] actually minimises the KLD in that particular case.

**Theorem 4.** For given labelled RFS densities  $\nu$  and  $\pi$ , PMF  $P_\varphi = P_\pi$ , label set  $L$  and vector densities  $\varphi(\cdot; \vec{L})$   $L' \subseteq \mathbb{L} \setminus L$  the solution to

$$\arg \min_{\varphi(\cdot; \vec{L})} D(\varphi \parallel \nu)$$

subject to  $\varphi \in [\pi]$  is

$$\varphi(x_{1:|L|}; \vec{L}) = \alpha(x_{1:|L|}; \vec{L}) \tilde{\pi}(\{x_1, \dots, x_{|L|}\}; \vec{L}) \quad (13)$$

$$\alpha(x_{1:|L|}; \vec{L}) = \frac{\nu(x_{1:|L|}; \vec{L})}{\tilde{\nu}(\{x_1, \dots, x_{|L|}\}; \vec{L})} \quad (14)$$

where the RFS density given the labels is

$$\tilde{\pi}(\{x_1, \dots, x_{|L|}\}; \vec{L}) = \sum_{p=1}^{|\vec{L}|!} \pi(\Gamma_{p,|L|}(x_{1:|L|}); \vec{L}) \quad (15)$$

and  $\Gamma_{p,t}(\cdot)$  indicates the  $p$ th permutation for  $t$  elements.

Theorem 4 is proved in Appendix C. We want to clarify that, according to (3)-(4),  $\varphi$  is characterised by  $P_\varphi$  and  $\varphi(\cdot; \vec{L})$   $L \subseteq \mathbb{L}$ . In Theorem 4, we are given all these densities except one, which is the one we optimise. Finally, the steps of the recursive optimisations are given in Algorithm 1.

---

#### Algorithm 1 Improved LMB approximation

---

**Input:** Initial labelled density  $\pi$ .

**Output:** LMB approximation  $\nu^*$ .

```

- Set  $\varphi^0 = \pi$ .
for  $n = 0$  to  $I_1 - 1$  do  $\triangleright I_1$  is the number of steps.
  - Calculate  $\nu^n$  using  $\varphi^n$  and Theorem 3.
  - Set  $\varphi^{n+1} = \varphi^n$ .
  for all  $L \subseteq \mathbb{L}$  do
    - Calculate  $\varphi^{n+1}(\cdot; \vec{L})$  using  $\nu^n$ ,  $\varphi^{n+1}(\cdot; \vec{L}')$ 
       $L' \neq L$  and Theorem 4.
  end for
end for
- Set  $\nu^* = \nu^{I_1-1}$ .
```

---

#### D. Illustrative example

In this section we consider an illustrative example to show how the previous algorithm for lowering the KLD works. Let us assume  $\kappa = 2$ ,

$$\pi(x_{1:2}; 1, 2) = \mathcal{N}\left(x_{1:2}; [10, 11]^T, \begin{bmatrix} \sigma_1^2 & \rho\sigma_1\sigma_2 \\ \rho\sigma_1\sigma_2 & \sigma_2^2 \end{bmatrix}\right) \quad (16)$$

$$\pi(x_1; 1) = \mathcal{N}(x_1; 10, \sigma_1^2) \quad (17)$$

Table I: PMF  $P_\pi$  for the illustrative example

	$\emptyset$	$\{1\}$	$\{2\}$	$\{1, 2\}$
Case 1	0.1	0.05	0.05	0.8
Case 2	0.1	0.3	0.3	0.3

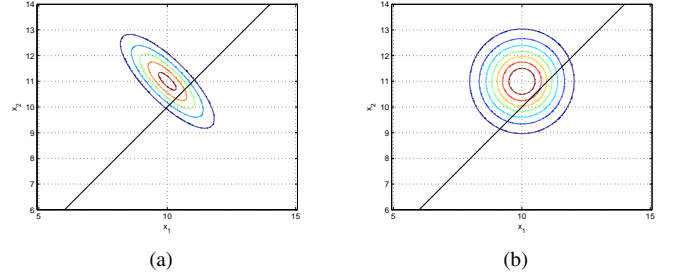


Figure 2: Joint PDF for labels 1, 2 for Cases 1 and 2: (a) initial PDF  $\varphi^0(\cdot; 1, 2)$  and (b) its best LMB approximation  $\nu^0(\cdot; 1, 2)$

$$\pi(x_1; 2) = \mathcal{N}(x_1; 11, \sigma_2^2) \quad (18)$$

where  $\sigma_1 = \sigma_2 = 1$ ,  $\rho = -0.8$ , and  $\mathcal{N}(x; \bar{x}, \Sigma)$  is the Gaussian PDF with mean  $\bar{x}$  and covariance matrix  $\Sigma$  evaluated at  $x$ . We consider two cases that differ in the PMF of the labels, see Table I. An important feature is that  $P_\pi(\{1, 2\})$  is considerably larger than the rest in Case 1.

The PDFs for labels 1 and 2 for the original PDF  $\varphi^0$  and its best LMB approximation  $\nu^0$  are shown in Figure 2. Both cases have the same PDF for labels 1 and 2 in the best LMB approximation because  $\pi(\cdot; 1)$ ,  $\pi(\cdot; 2)$  correspond with the marginal PDFs of  $\pi(\cdot; 1, 2)$ , although this is not necessarily this case. It should be noted that in both cases,  $\varphi^n(\cdot; 1) = \pi(\cdot; 1)$  and  $\varphi^n(\cdot; 2) = \pi(\cdot; 2) \forall n$ . This is due to the fact that the previous recursion only performs changes in the PDFs that represent more than one target. As we iterate, the KLD gets lower as shown in Table II. The PDFs for labels 1 and 2 for  $\varphi^5$  and  $\nu^5$  in Case 1 are shown in Figure 3. It is clear that there are considerable differences between  $\varphi^0$  and  $\varphi^5$  that enable the significant lowering of the KLD, although they contain the same information regarding the corresponding unlabelled set. In case 2, the KLD is also reduced but much less, see Table II. The reason behind this behaviour is that, in Case 1, it is highly likely that two targets exist and the weight of the PDFs with labels with a single target are quite low. Therefore, the resulting optimisation is quite similar to the case in which there are always two targets, see [31]. On the contrary, in Case 2, the single target PDFs have a more important weight and the best LMB approximation is clearly influenced by  $\pi(\cdot; 1)$  and  $\pi(\cdot; 2)$  so the KLD cannot be reduced much. Nevertheless, the recursion always ensures that the new PDFs are more accurately approximated as LMB than the original ones.

Table II: KLD of  $\nu^n$  from  $\varphi^n$

Iteration number $n$	0	1	2	3	4	5
Case 1	0.542	0.467	0.408	0.382	0.375	0.374
Case 2	0.184	0.164	0.160	0.159	0.159	0.159

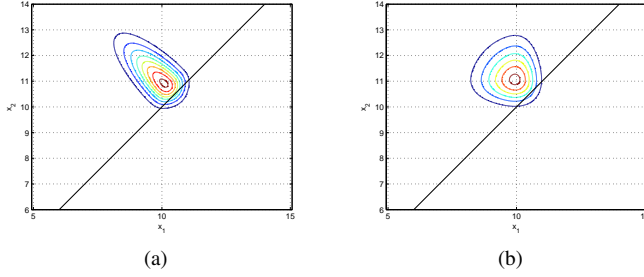


Figure 3: Joint PDF for labels 1, 2 for Case 1: (a) PDF  $\varphi^5(\cdot; 1, 2)$  and (b) its best LMB approximation  $\nu^5(\cdot; 1, 2)$

#### IV. LABELLED MULTI-BERNOULLI PARTICLE FILTER

In this section, we describe the generalised parallel partition (GPP) particle filter, which is a generalisation of the parallel partition (PP) particle filter [4, Sec. III] that accounts for target births and deaths. The PP-PF corresponds to the GPP-PF with a known and fixed number of targets. Note that for fixed and known number of targets, a vector representation of the multitarget state is equivalent to a labelled RFS [30], so, in this case, an LMB RFS density is equivalent to a density on a multitarget vector state with independent targets. In Section IV-A, we provide the posterior PDF and explain the use of an auxiliary variable in GPP-PF. The importance density to sample the posterior and the resulting particle weights are provided in Section IV-B.

##### A. Posterior density

We assume

- A2 The posterior at the previous time step is LMB with existence probabilities  $p_j^-$  and densities  $\pi^-(\cdot; j)$   $j \in \{1, \dots, \kappa^-\}$ .
- A3 The PDF of the new born targets is LMB with existence probabilities  $p_j$  and densities  $\eta(\cdot; j)$   $j \in \{\kappa^- + 1, \dots, \kappa\}$ .

We recall that we assume without loss of generality that  $\mathbb{L} = \{1, \dots, \kappa\}$ . In a PF, we draw  $N$  particles  $\{\mathbf{X}^1, \dots, \mathbf{X}^N\}$  from an importance density, where  $\mathbf{X}^i$  represents the  $i$ th particle, and in order to evaluate the weight of the  $i$ th particle we need to evaluate  $\pi(\mathbf{X}^i)$ . Note that these particles are usually stored in matrices in a computer implementation [5, Sec. III.A]. In the following, we represent the posterior PDF using decomposition (3)-(4). For evaluating the posterior for a specific particle, we find it useful to denote by  $\vec{L}^i$  and  $x_{1:|\vec{L}^i|}^i$  the vector of labels of  $\mathbf{X}^i$  arranged in ascending order and  $x_{1:|\vec{L}^i|}^i$  their corresponding states [5]. Therefore,

$$\pi(\mathbf{X}^i) = P_\pi(L^i) \pi(x_{1:|\vec{L}^i|}^i; \vec{L}^i). \quad (19)$$

Under A2 and considering Section III-B, the posterior at the previous time is characterised by

$$P_{\pi^-}(L) = \prod_{j=1}^{\kappa^-} (1 - p_j^-) \prod_{j=1}^{|L|} \frac{p_{L_j}^-}{1 - p_{L_j}^-} \quad (20)$$

$$\pi^-(x_{1:|L|}; \vec{L}) = \prod_{j=1}^{|L|} \pi^-(x_j; L_j) \quad (21)$$

where  $L_j$  indicates the  $j$ th component of  $\vec{L} = (L_1, \dots, L_{|L|})$ .

Let us assume that we have a Monte Carlo (MC) approximation of the posterior at the previous time such that

$$\pi^-(x_{1:|L|}; \vec{L}) \propto \prod_{j=1}^{|L|} \sum_{i=1}^{N_{L_j}^-} \delta(x_j - x_{L_j}^{-i}) \quad (22)$$

where  $\delta(\cdot)$  is the Dirac delta,  $x_{L_j}^{-i}$  is the  $i$ th particle and  $N_{L_j}^-$  is the number of particles of density  $\pi^-(\cdot; L_j)$  and the weights are even. Then, making the usual assumptions that targets move independently with single target transition density  $g(\cdot|\cdot)$  and probability of survival  $\gamma$ , the prior PDF  $\xi$  of the surviving targets, which is also called the predicted PDF of the surviving targets, is also LMB with [13]

$$P_\xi(L) = \prod_{j=1}^{\kappa^-} (1 - p_j) \prod_{j=1}^{|L|} \frac{p_{L_j}}{1 - p_{L_j}} \quad (23)$$

$$\xi(x_{1:|L|}; \vec{L}) \propto \prod_{j=1}^{|L|} \sum_{i=1}^{N_{L_j}^-} g_{L_j}^i(x_j) \quad (24)$$

where

$$p_{L_j} = \gamma \cdot p_{L_j}^- \quad (25)$$

$$g_j^i(\cdot) = g(\cdot|x_j^{-i}) \quad j \in \{1, \dots, \kappa^-\}. \quad (26)$$

Under A3, the prior PDF  $\omega$  at the current time step, which is the predicted PDF of the surviving targets and the new born targets, is also LMB with [13]

$$P_\omega(L) = \prod_{j=1}^{\kappa} (1 - p_j) \prod_{j=1}^{|L|} \frac{p_{L_j}}{1 - p_{L_j}} \quad (27)$$

$$\omega(x_{1:|L|}; \vec{L}) \propto \prod_{j=1}^{|L|} \sum_{i=1}^{N_{L_j}^-} g_{L_j}^i(x_j) \quad (28)$$

where

$$g_j^i(\cdot) = \eta(\cdot; j) \quad j \in \{\kappa^- + 1, \dots, \kappa\} \quad (29)$$

$$N_{L_j}^- = N \quad j \in \{\kappa^- + 1, \dots, \kappa\}. \quad (30)$$

Note that in (28) we write the PDFs of the new born targets also as a mixture of PDFs to deal with surviving and new born targets jointly with the same notation. Applying Bayes' rule, we obtain the posterior [5]

$$\begin{aligned} \pi(x_{1:|L|}; \vec{L}) P_\pi(L) &\propto \ell(\{x_1, \dots, x_{|L|}\}) \\ &\times P_\omega(L) \prod_{j=1}^{|L|} \sum_{i=1}^{N_{L_j}^-} g_{L_j}^i(x_j). \end{aligned} \quad (31)$$

As in the PP method [4], we use an auxiliary vector  $a_{1:|L|} = (a_1, \dots, a_{|L|})$  such that we write

$$\pi(x_{1:|L|}, a_{1:|L|}; \vec{L}) P_\pi(L) \propto \ell(\{x_1, \dots, x_{|L|}\})$$

$$\times P_{\omega}(L) \prod_{j=1}^{|L|} g_{L_j}^{a_j}(x_j) \quad (32)$$

where  $a_j \in \{1, \dots, N_{L_j}^-\}$  and each component of  $a_{1:|L|}$  is an index on the mixture in (31). In other words, in (32), the state  $x_j$  of target  $j$  comes from particle  $a_j$  at the previous time step. The auxiliary vector is quite useful because it lowers the computational complexity by removing the sum in (31) and allows for subparticle crossover [4]. As illustrated in [4, Fig. 1], subparticle crossover refers to the fact that a (multitarget) particle of the posterior can be formed by propagating subparticles, part of the multitarget particle that represents a target, that belonged to different particles at the previous time step. As expected, integrating out  $a_{1:|L|}$  in (32), we obtain (31). In general, samples from (32) cannot be obtained directly, so we proceed to describe an importance density to draw samples from.

### B. Importance density and particle weights

The predicted state of the target with label  $j$  is<sup>1</sup>

$$\hat{x}_j = \frac{1}{N_j^{k-1}} \sum_{i=1}^{N_j^-} E[g_j^i(x)] \quad j \in \{1, \dots, \kappa\}. \quad (33)$$

The set of predicted states with labels in  $L$  is

$$\hat{X}_L = \{\hat{x}_{L_1}, \dots, \hat{x}_{L_{|L|}}\}.$$

We first write the importance density  $q$  in terms of its decomposition (3)-(4) and then we explain it:

$$P_q(L) \propto P_{\omega}(L) \ell(\hat{X}_L) \quad (34)$$

$$q(x_{1:|L|}, a_{1:|L|}; \vec{L}) = \prod_{j=1}^{|L|} \frac{g_{L_j}^{a_j}(x_j) \ell(\{x_j\} \cup \hat{X}_{L \setminus L_j})}{\beta_{L_j}} \quad (35)$$

$$\beta_{L_j} = \sum_{a_j=1}^{N_{L_j}^-} \int g_{L_j}^{a_j}(x_j) \ell(\{x_j\} \cup \hat{X}_{L \setminus L_j}) dx_j \quad (36)$$

where  $L \setminus L_j$  indicates label set  $L$  without label  $L_j$  and  $\beta_{L_j}$  is a normalising constant. Sampling from  $q$  is performed in two steps. First, we obtain  $N$  samples  $L^1, \dots, L^N$  from (34). As  $L$  is a discrete set, this task can be performed easily. Each of these samples contains the labels of the targets whose states have to be sampled to obtain the final particles from the posterior. An important characteristic of  $P_q$  is how it takes into account the current measurement and target states. It uses the predicted target states for each configuration of labels (hypotheses), represented by  $\hat{X}_L$ , and the current measurement, included in  $\ell(\hat{X}_L)$ , to draw possible existences, see Figure 4. This way, we draw more particles with hypotheses which are predicted to have a higher posterior weight.

<sup>1</sup>If we cannot obtain  $E[g_j^i(x)]$  in closed-form, we can instead draw  $\hat{x}_j$  as a sample from  $g_j^i(\cdot)$  as discussed in [28] for the PP method or in [34] for the auxiliary PF.

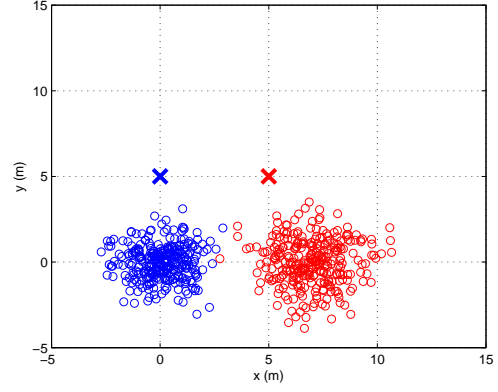


Figure 4: Illustration of the sampling of the label set. The position particles of two targets at the previous time step are shown as blue and red circles. The crosses denote the predicted positions at the current time step for each target, which are obtained using these particles and the dynamic model, see (33). Based on these predicted positions and the current measurement, we sample the label PMF using (34).

Once we have obtained  $N$  samples  $L^1, \dots, L^N$  from (34), we have  $H$  different label sets  $\hat{L}^1, \dots, \hat{L}^H$  and  $N_{\hat{L}^h}$  particles with label set  $\hat{L}^h$ . Then, for all the particles with label set  $\hat{L}^h$ , we use (35) to obtain  $N_{\hat{L}^h}$  samples of the target states. The density (35) is the importance density of the PP method given the label set  $\hat{L}^h$ . How target state sampling is performed and the properties of the PP method are thoroughly discussed in [4, Sec. III]. Target states are sampled independently, this is why there is a product over the target index  $j$ , and the other target states are taken into account in the likelihood by their predicted states, see (33) and Figure 4. It should be noted that in (35), we include the normalising constant  $\beta_{L_j}$ . The reason behind this is that the importance density (35) for each  $\hat{L}^h$  is different so we have to consider the normalising constants in the final particle weight. The normalising constants are approximated as [15]

$$\beta_{L_j} \approx \frac{1}{N_{L_j}^-} \sum_{i=1}^{N_{L_j}^-} \ell(\{\hat{x}_j^i\} \cup \hat{X}_{L \setminus L_j}) \quad (37)$$

where  $\hat{x}_j^i \sim g_{L_j}^i(\cdot)$ .

The final particles are represented by  $\{(L^1, x_{1:|L^1|}^1, a_{1:|L^1|}^1), \dots, (L^N, x_{1:|L^N|}^N, a_{1:|L^N|}^N)\}$ . Using (32) and (34)-(36), the weight of the  $i$ th particle becomes

$$w^i \propto \frac{\ell(\{x_1^i, \dots, x_{|L^i|}^i\})}{\ell(\hat{X}_{L^i}) \prod_{j=1}^{|L^i|} b_j(L^i, x_j^i)} \quad (38)$$

$$b_j(L^i, x_j^i) = \frac{\ell(\{x_j^i\} \cup \hat{X}_{L^i \setminus L_j^i})}{\beta_{L_j^i}}. \quad (39)$$

where  $L_j^i$  denotes the  $j$ th component in ascending order of  $L^i$ , i.e.,  $\vec{L}^i = (L_{L_1^i}^i, \dots, L_{L_{|L^i|}^i}^i)$ .

The steps for drawing samples in the GPP method are provided in Algorithm 2. Finally, in order to be able to perform the filtering recursion, at the next time step, we need a prior of the form (28). This can be achieved by first performing

resampling to obtain evenly distributed weights and directly approximate the current particle approximation as LMB using Theorem 3. This results in an LMB approximation such that the particles and existence probability for the target with label  $j$  are:

$$\{x_j^1, \dots, x_j^{N_j}\} = \{x_p^i : L_p^i = j, p \in \{1, 2, \dots, |L^i|\}\} \quad (40)$$

$$p_j = \frac{N_j}{N} \quad (41)$$

where (40) simply takes the particles which have label  $j$  and (41) indicates that the probability of existence of the  $j$ target is proportional to the number of particles that contain it.

If we are not interested in target labels instead of using (40)-(41), we can use the label switching improvement algorithm explained in Section V. The overall steps of the PF are indicated in Algorithm 3.

---

#### Algorithm 2 GPP particle filter subroutine

---

**Input:** Existence probability  $p_j^-$  and  $N_j^-$  particles  $\{x_j^{-1}, \dots, x_j^{-N_j^-}\}$  for  $j = \{1, \dots, \kappa^-\}$ , which represent (28).

**Output:**  $N$  particles with even weights  $\left\{ \left( L^1, x_{1:|L^1|}^1, a_{1:|L^1|}^1 \right), \dots, \left( L^N, x_{1:|L^N|}^N, a_{1:|L^N|}^N \right) \right\}$ , which approximate (32).

- Calculate  $p_j = \gamma \cdot p_j^-$  for  $j = \{1, \dots, \kappa^-\}$ .
- Calculate  $\hat{x}_j$  for  $j = \{1, \dots, \kappa\}$  using (33).  $\triangleright$  This step includes new born targets
- Obtain  $N$  samples  $L^1, \dots, L^N$  from (34).
- From  $L^1, \dots, L^N$ , obtain the different label sets  $\dot{L}^1, \dots, \dot{L}^H$  and the number  $N_{\dot{L}^h}$  of particles with  $\dot{L}^h$ .
- Set  $r = 1$   $\triangleright$   $r$  is an index on the particles of the posterior.
- $\triangleright$  Go through all the sampled label sets.

**for**  $h = 1$  to  $H$  **do**

$\triangleright$  Go through the targets indicated by  $\dot{L}^h$ .

**for**  $j = 1$  to  $|\dot{L}^h|$  **do**

$\triangleright$  Draw the particles for the  $j$ th target in  $\dot{L}^h$ .

**for**  $l = 1$  to  $N_{\dot{L}^h}^-$  **do**

- Obtain a sample  $\tilde{x}_j^l \sim g_{\dot{L}^h}^l(x_j)$ .
- Calculate  $c(\tilde{x}_j^l) = \ell(\{\tilde{x}_j^l\} \cup \hat{X}_{\dot{L}^h \setminus \dot{L}^h})$ .

**end for**

- Normalise  $c(\tilde{x}_j^l)$  to sum to one over  $l = 1$  to  $N_{\dot{L}^h}^-$ .

**for**  $l = 1$  to  $N_{\dot{L}^h}$  **do**

- $\triangleright$  Resampling stage for the  $j$ th target in  $\dot{L}^h$ .
- Sample an index  $p$  from the distribution defined by  $c(\tilde{x}_j^l)$  over  $i = 1$  to  $N_{\dot{L}^h}^-$ .
- Set  $x_j^r = \tilde{x}_j^p$ ,  $L_j^r = \dot{L}^h$  and  $a_j^r = p$ .
- Set  $b_j(\dot{L}^h, x_j^r) = N_{\dot{L}^h}^- \cdot c(\tilde{x}_j^p)$ .
- Set  $r = r + 1$ .

**end for**

**end for**

**end for**

$\triangleright$  Weight calculation

**for**  $i = 1$  to  $N$  **do**

- Calculate the weight  $w^i$  using (38).

**end for**

- Perform resampling to obtain even particle weights.
- 

## V. LABEL SWITCHING IMPROVEMENT USING MCMC

In this section, we apply the label switching algorithm to improve the LMB approximation described in Section III to

---

#### Algorithm 3 LMB particle filter algorithm

---

**Input:** Existence probability  $p_j^-$  and  $N_j^-$  particles  $\{x_j^{-1}, \dots, x_j^{-N_j^-}\}$  for  $j = \{1, \dots, \kappa^-\}$ , which represent (28).

**Output:** Existence probability  $p_j$  and  $N_j$  particles  $\{x_j^1, \dots, x_j^{N_j}\}$  for  $j = \{1, \dots, \kappa\}$ , which approximate (32) as LMB.

- Use Algorithm 2 to obtain  $N$  particles with even weights  $\left\{ \left( L^1, x_{1:|L^1|}^1, a_{1:|L^1|}^1 \right), \dots, \left( L^N, x_{1:|L^N|}^N, a_{1:|L^N|}^N \right) \right\}$ , which approximate (32).

$\triangleright$  Obtain LMB approximation

**if** Label switching improvement **then**

$\triangleright$  Useful when targets get in close proximity

- Use Algorithm 4 to obtain  $p_j$  and  $N_j$  particles  $\{x_j^1, \dots, x_j^{N_j}\}$

for  $j = \{1, \dots, \kappa\}$ .

**else**

- Use (40)-(41) to obtain  $p_j$  and  $N_j$  particles  $\{x_j^1, \dots, x_j^{N_j}\}$

for  $j = \{1, \dots, \kappa\}$ .

**end if**

---

the output of the PF developed in the previous section, see Figure 1. More specifically, we use MCMC to approximate the sequence  $\varphi^0 = \pi, \nu^0, \varphi^1, \nu^1 \dots$  indicated in Algorithm 1. The resulting algorithm is called improved LMB MCMC (ILMB-MCMC).

First, we calculate the RFS density given the labels, which is given by (15), using the posterior (31) to obtain

$$\begin{aligned} \tilde{\pi}(\{x_1, \dots, x_{|L|}\}; \vec{L}) &\propto \ell(\{x_1, \dots, x_{|L|}\}) \\ &\times \sum_{p=1}^{|L|!} \prod_{j=1}^{|L|} \sum_{i=1}^{N_{\dot{L}^j}^-} g_{\dot{L}^j}^i(x_{\phi_{|L|,p,j}}) \end{aligned} \quad (42)$$

where  $[\phi_{t,p,1}, \dots, \phi_{t,p,t}]^T \in \{1, \dots, t\}^t$  represents the permutations of vector  $[1, \dots, t]^T$ . We recall from Theorem 4 that any density  $\varphi^n(\cdot; \vec{L})$  of the recursion can be written as  $\varphi^n(\cdot; \vec{L}) = \alpha^n(\cdot; \vec{L}) \tilde{\pi}(\cdot; \vec{L})$ . Using the auxiliary vector  $a_{1:|L|}$ , which was defined in (32), we get

$$\begin{aligned} \varphi^n(x_{1:|L|}, a_{1:|L|}; \vec{L}) &\propto \alpha^n(x_{1:|L|}; \vec{L}) \ell(\{x_1, \dots, x_{|L|}\}) \\ &\times \sum_{p=1}^{|L|!} \prod_{j=1}^{|L|} g_{\dot{L}^j}^{a_j} (x_{\phi_{|L|,p,j}}) \end{aligned} \quad (43)$$

From the MC approximation  $\left\{ \left( L^1, x_{1:|L^1|}^1, a_{1:|L^1|}^1 \right), \dots, \left( L^N, x_{1:|L^N|}^N, a_{1:|L^N|}^N \right) \right\}$  to the density  $\pi$ , which is obtained using the GPP PF, we can directly get the PMF  $P_\pi$  and rearrange the particles to get the PDFs of the states and auxiliary variables given the label set for the initial PDF:

$$P_\pi(L) = N_L/N \quad (44)$$

$$\begin{aligned} \varphi^0(x_{1:|L|}, a_{1:|L|}; \vec{L}) &\propto \sum_{i=1}^{N_L} \delta(a_{1:|L|} - a_{1:|L|}^{L,i}) \\ &\times \delta(x_{1:|L|} - x_{1:|L|}^{L,i,0}) \end{aligned} \quad (45)$$

where  $N_L$  is the number of particles with label set  $L$  and  $(x_{1:|L|}^{L,i,n}, a_{1:|L|}^{L,i})$  denotes the  $i$ th particle of the PDF  $\varphi^n(\cdot; \vec{L})$ .



The recursion can be performed if, given an MC approximation to  $\varphi^n(\cdot; \vec{L})$ , we can obtain an MC approximation to  $\varphi^{n+1}(\cdot; \vec{L}) \forall L$ . In order to get samples from  $\varphi^{n+1}(\cdot; \vec{L})$ , see (43), we need to find  $\alpha^{n+1}(\cdot)$  using Theorems 3 and 4. In Section V-A, we explain how to approximate  $\alpha^{n+1}(\cdot)$ . In Section V-B, we describe the MCMC algorithm to obtain samples from (43) once  $\alpha^{n+1}(\cdot)$  is obtained.

#### A. Approximation of $\alpha^{n+1}(\cdot)$

In order to be able to run the MCMC algorithm that gives samples from  $\varphi^{n+1}(\cdot; \vec{L})$ , we need to calculate  $\alpha^{n+1}(\cdot)$  based on the MC approximation to  $\varphi^n(\cdot; \vec{L}) \forall \vec{L}$  and Theorems 3 and 4.

Using (44) and (45) and Theorem 3, we get

$$\nu^n(x_1; j) = \frac{1}{N_j} \sum_{L \ni j} \sum_{i=1}^{N_L} \delta(x_1 - x_j^{L,i,n}) \quad (46)$$

$$N_j = \sum_{L \ni j} N_L \quad (47)$$

where  $x_j^{L,i,n}$  indicates the  $i$ th particle of the target with label  $j$  in  $\varphi^n(\cdot; \vec{L})$ . Theorem 4 provides  $\alpha^{n+1}(\cdot)$  based on  $\nu^n(\cdot; \vec{L}) = \prod_{j=1}^{|L|} \nu^n(\cdot; L_j)$ . However, we cannot evaluate  $\nu^n(\cdot; \vec{L})$  directly because the PDF is represented by Dirac delta functions. We solve this by approximating (46) as a Gaussian PDF

$$\nu^n(x_1; j) \approx \mathcal{N}(x_1; \bar{x}_j^n, P_j^n) \quad (48)$$

where  $\bar{x}_j^n$  and  $P_j^n$  are obtained by moment matching

$$\bar{x}_j^n = \frac{1}{N_j} \sum_{L \ni j} \sum_{i=1}^{N_L} x_j^{L,i,n} \quad (49)$$

$$P_j^n = \frac{1}{N_j} \sum_{L \ni j} \sum_{i=1}^{N_L} (x_j^{L,i,n} - \bar{x}_j^n) (x_j^{L,i,n} - \bar{x}_j^n)^T. \quad (50)$$

This approximation is accurate enough to improve the LMB approximation in the examples of [31] and Section VI. Otherwise, we can regularise (46) [9]. Using Theorem 4, we get

$$\alpha^{n+1}(x_{1:|L|}; \vec{L}) \approx \frac{\prod_{j=1}^{|L|} \nu^n(x_j; L_j)}{\sum_{p=1}^{|L|!} \prod_{j=1}^{|L|} \nu^n(x_{\phi_{|L|,p,j}}; L_j)}. \quad (51)$$

#### B. MCMC steps to improve the LMB approximation

In the previous subsection, we indicated how to approximate  $\alpha^{n+1}(\cdot)$  based on the MC approximations to  $\varphi^n(\cdot; \vec{L})$ . In this section, we design an MCMC algorithm to sample from  $\varphi^{n+1}(\cdot; \vec{L})$ , which is given by (43). In principle, we can use any MCMC algorithm, e.g., Metropolis-Hastings [10]. Nevertheless, we can perform the MCMC sampling more efficiently due to the characteristics of the PDF (43).

In any MCMC algorithm, we evaluate the target PDF up to a proportionality constant. When we evaluate (43)

for a state  $(x_{1:|L|}, a_{1:|L|})$ , we compute the same terms we would calculate to evaluate (43) for any of its permutations  $(\Gamma_{p,|L|}(x_{1:|L|}), a_{1:|L|})$   $p = 1, \dots, |L|!$ . Therefore, as evaluating (43) for all the permutations comes at practically no extra cost, it is of high interest to develop an MCMC algorithm that accounts for all the permutations at the same step.

Conditioned on  $a_{1:|L|}$ , the proposed MCMC algorithm performs moves in the state. The algorithm requires the specification of a transition rule w.r.t. which the target PDF is invariant [10]. For a given  $x_{1:|L|}$ , we propose the following transition rule to the next state  $y_{1:|L|}$ . First, we sample  $\tilde{x}_{1:|L|}$  from a density  $q(\tilde{x}_{1:|L|} | x_{1:|L|}) = \prod_{j=1}^{|L|} q'(\tilde{x}_j | x_j)$ . Then, we set  $y_{1:|L|} = \Gamma_{p,|L|}(x_{1:|L|})$  or  $y_{1:|L|} = \Gamma_{p,|L|}(\tilde{x}_{1:|L|})$  with probabilities  $\beta'_p$  and  $\tilde{\beta}'_p$  for  $p = 1, \dots, t!$

$$y_{1:|L|} = \begin{cases} \Gamma_{p,|L|}(x_{1:|L|}) & \beta'_p = \frac{\beta_p}{\sum_{p=1}^{t!} (\beta_p + \tilde{\beta}_p)} \\ \Gamma_{p,|L|}(\tilde{x}_{1:|L|}) & \tilde{\beta}'_p = \frac{\tilde{\beta}_p}{\sum_{p=1}^{t!} (\beta_p + \tilde{\beta}_p)} \end{cases} \quad (52)$$

where

$$\beta_p = \varphi^{n+1}(\Gamma_{p,|L|}(x_{1:|L|}), a_{1:|L|}; \vec{L}) \quad (53)$$

$$\tilde{\beta}_p = \varphi^{n+1}(\Gamma_{p,|L|}(\tilde{x}_{1:|L|}), a_{1:|L|}; \vec{L}) \quad (54)$$

and  $\varphi^{k,n+1}(\cdot)$  is given by (43). It is shown in Appendix D that this transition rule is invariant if  $q'(\cdot | \cdot)$  is symmetric and therefore leads to a valid MCMC algorithm.

To sum up, the ILMB-MCMC has three design parameters: the number  $I_1$  of steps of the recursion explained in Section III, the number  $I_2$  of steps that allow for the MCMC burn-in period to get samples from  $\varphi^{k,n}(\cdot)$  and the transition density  $q(\cdot | x_{1:|L|})$ . Its steps are given in Algorithm 4.

#### C. Discussion

In this paper, we have developed a PF, which is called GPP, that approximates the labelled posterior based on an LMB posterior at the previous time step. This PF can be used on its own without the need of any MCMC or label switching improvement algorithm. Nevertheless, if we are interested in the unlabelled posterior, we can make use of the recursion explained in Section III to improve the LMB approximation. Section V explains an algorithm based on MCMC to approximate the recursion in Section III. The complexity of the MCMC algorithm depends on the number of targets through the number of possible permutations. Nevertheless, the benefits of the MCMC algorithm are only expected to happen when targets get in close proximity and then separate because of the mixing of the labels [7]. As a result, in practice, we should only apply the MCMC algorithm for targets in close proximity, e.g., by clustering [4], [21], [27].

We also want to mention that, in some cases, the dimensionality of the PF can be reduced by applying Rao-Blackwellisation [21]. In this case, measurement nonlinearities can only be a function of some elements of the state, e.g., they apply to the position but not the velocity. Function  $\alpha^n(\cdot)$  in (43) would prevent the use of Rao-Blackwellisation even when the measurement and dynamic models allow for it. This could be sorted out by looking for a



---

**Algorithm 4** MCMC algorithm to improve the LMB approximation (ILMB-MCMC)

---

**Input:**  $N$  particles with even weights  
 $\left\{ \left( L^1, x_{1:|L^1|}^1, a_{1:|L^1|}^1 \right), \dots, \left( L^N, x_{1:|L^N|}^N, a_{1:|L^N|}^N \right) \right\}$ , which approximate (32).

**Output:** Existence probability and  $N_j$  particles which represent the density of the target with label  $j$ .

- Obtain  $P_\pi$  using (44).

**for all**  $L$  **do**

- Obtain  $\left( x_{1:|L|}^{L,i,0}, a_{1:|L|}^{L,i} \right)$ , see (45).

**end for**

**for**  $n = 0$  to  $I_1 - 1$  **do**

- Calculate  $\bar{x}_j^n$  and  $P_j^n$  for  $j \in \{1, \dots, \kappa\}$  using (49) and (50).

**for all**  $L$  **do**

- Calculate  $\alpha^{n+1} \left( \cdot; \bar{L} \right)$  using (51).

- Set  $x_{1:|L|}^{L,i,n+1} = x_{1:|L|}^{L,i,n}$   $i = 1, \dots, N_L$ .

**for**  $h = 0$  to  $I_2 - 1$  **do**

**for**  $i = 1$  to  $N_L$  **do**

- Sample  $\tilde{x}_{1:|L|}^i$  from  $q \left( \cdot \mid x_{1:|L|}^{L,i,n+1} \right)$ .

- Use  $x_{1:|L|}^{L,i,n+1}$  and  $\tilde{x}_{1:|L|}^i$  to calculate  $\beta_p$  and  $\tilde{\beta}_p$  by

(53), (54) and (43).

- Select  $y_{1:|L|}$  according to (52).

- Set  $x_{1:|L|}^{L,i,n+1} = y_{1:|L|}$ .

**end for**

**end for**

**end for**

**end for**

- Obtain the existence probabilities for  $j = \{1, \dots, \kappa\}$  using  $P_\pi$  and Theorem 3.

---

labelled PDF within the unlabelled RFS family that allows for Rao-Blackwellisation. Nevertheless, the development of this idea is beyond the scope of this paper.

## VI. NUMERICAL SIMULATIONS

In this section, we evaluate the performances of the GPP method and the ILMB-MCMC algorithm in MTT using a sensor network. We analyse two examples. In the first one, we set aside the problem of target births and study the performance of the proposed algorithms when targets get in close proximity and then separate. The second example considers target births.

Both examples are based on the following dynamic/measurement models. In this section, we use a superindex to denote the time step  $k$ . The state vector of the  $j$ th target at time  $k$  is  $x_j^k = [p_{x,j}^k, \dot{p}_{x,j}^k, p_{y,j}^k, \dot{p}_{y,j}^k]^T$ . The dynamic model of the target is the nearly-constant velocity model:

$$x_j^{k+1} = F x_j^k + v^k \quad (55)$$

$$F = I_2 \otimes \begin{pmatrix} 1 & \tau \\ 0 & 1 \end{pmatrix} \quad (56)$$

where  $\otimes$  is the Kronecker product,  $I_n$  is the identity matrix of size  $n$  and  $v^k$  is the process noise at time  $k$ . The process noise is zero-mean Gaussian distributed with covariance matrix

$$Q = q I_2 \otimes \begin{pmatrix} \tau^3/3 & \tau^2/2 \\ \tau^2/2 & \tau \end{pmatrix} \quad (57)$$

where  $q$  is a parameter of the model and  $\tau$  is the sampling period.

There are  $M = 252$  sensors, so the measurement vector at time  $k$  is  $z^k = [z_1^k, \dots, z_M^k]^T$  where  $z_j^k$  is the measurement of the  $j$ th sensor at time  $k$ . Sensor  $m$  is located at  $[\xi_{x,m}, \xi_{y,m}]^T$  and measures an acoustic signal emitted by the target with measurement model

$$z_m^k = \sqrt{\sum_{j=1}^t h_m(x_j^k)} + w_m^k \quad (58)$$

where

$$h_m(x_j^k) = \begin{cases} \frac{P_0 d_0^2}{d_m^2(x_j^k)} & d_m^2(x_j^k) > d_0^2 \\ P_0 & d_m^2(x_j^k) \leq d_0^2 \end{cases} \quad (59)$$

and  $w_m^k$  is an independent zero-mean Gaussian noise with variance  $\sigma_s^2$ ,  $P_0$  is the saturation power,  $d_0$  is the distance at which this saturation power is produced and  $d_m^2(x_j^k)$  is the square distance from the target  $x_j^k$  to the  $m$ th sensor

$$d_m^2(x_j^k) = (p_{x,j}^k - \xi_{x,m})^2 + (p_{y,j}^k - \xi_{y,m})^2. \quad (60)$$

Measurement equation (58) models the amplitude of the received acoustic signal at a sensor from incoherently emitting targets [35] and is not superpositional so filters such as [17], [18] cannot be used.

### A. Targets in close proximity for a long time

The main objective of this section is to analyse algorithm performances when targets get in close proximity for a sufficiently long time and then separate. In this case, there is mixing of the labels so the labelling switching algorithm based on MCMC is expected to be useful. In order to study this case in an isolated way, we assume that there are no target births

We have implemented the GPP method followed by a usual MCMC algorithm (U-MCMC GPP) after resampling and the GPP method with the ILMB-MCMC algorithm. The U-MCMC algorithm corresponds to the Metropolis-Hastings algorithm with 20 steps [9]. We have implemented 3 versions of ILMB-MCMC GPP that differ in their parameters  $I_1$  and  $I_2$ , see Table III. They have roughly the same number of MCMC steps, indicated by  $I_1 \times I_2$ , but different number  $I_1$  of iterations in the sequence of Section III. We recall that U-MCMC improves sample diversity while ILMB-MCMC improves sample diversity and the required LMB approximation. Therefore, we approximately use the same number of MCMC steps in both methods such that the improvement is not due to sample diversity but improvement in LMB approximation, which is what we want to assess. U-MCMC and ILMB-MCMC use the transition density

$$q'(\tilde{x}_j^k | x_j^k) = \mathcal{N}(\tilde{x}_j^k; x_j^k, Q). \quad (61)$$

We compare these algorithms with the two-layer parallel partition (PP) PF, which has been demonstrated to outperform a variety of filters in track-before-detect applications [4]. For this filter, we use the same parameters as in [4]. We have also implemented the sampling importance resampling PF (SIR-PF) [36].

Table III: ILMB-MCMC GPP parameters

Version	$I_1$	$I_2$
1	1	20
2	2	10
3	3	6

Table IV: Parameters of the simulation

Parameter	$\tau$	$q$	$P_0$	$\sigma_s^2$	$d_0$	$\gamma$
Value	0.5 s	3.24 m <sup>2</sup> /s <sup>3</sup>	15.85 W	1	20 m	0.99

The estimation error is evaluated using the optimal sub-pattern assignment (OSPA) metric with  $c = 120$  m, Euclidean distance and  $p = 2$  [37]. In order to estimate target states, we first obtain the most likely cardinality from the PF. If the cardinality is known and  $c \rightarrow \infty$ , the minimum MSOSPA (MMSOSPA) estimator corresponds to the mean of the unlabelled RFS density in a Voronoi region [30], [38]. Therefore, we integrate out the labels of the particles and then use  $k$ -means clustering on the particles as in [20] as an approximation to the MMSOSPA estimator. Importantly, this clustering is only performed to estimate target states, it does not affect the approximation of the posterior PDF at the following time steps as done in [20].

The target trajectories are shown in Figure 5. The target with blue trajectory in Figure 5 dies at time step 85 while the other two targets are alive at all time steps. The algorithms' performances are evaluated based on Monte Carlo simulation with 500 runs. The simulation parameters are those given in Table IV, where we recall that  $\gamma$  is the probability of survival. The prior PDF of the  $j$ th target at time step 0 is  $\mathcal{N}(\bar{x}_j^0; \bar{\Sigma}_j^0)$  where  $\bar{x}_j^0$  and  $\bar{\Sigma}_j^0$  are the mean and covariance matrix of the  $j$ th target at time 0. In each Monte Carlo run,  $\bar{x}_j^0$  is drawn from Gaussian distribution whose mean is the true target position and  $\bar{\Sigma}_j^0 = 100I_4$ . In addition, the filters are also initiated with another target, which does not exist, whose PDF is Gaussian with mean  $\bar{x}_j^0 = [600, 0, 200, 0]^T$  and covariance  $100I_4$  in international system units. The initial probability of existence of all targets is set to one.

First, we assess the filters' performances using 500 particles except for the SIR-PF, which uses 10000 particles. The aim

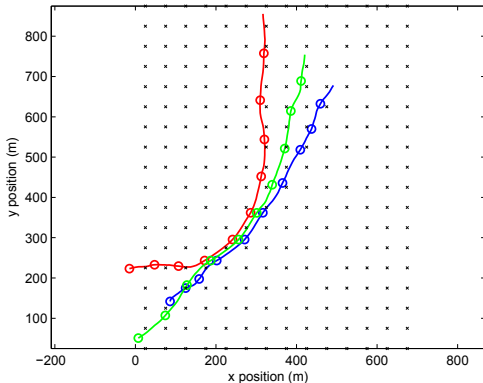
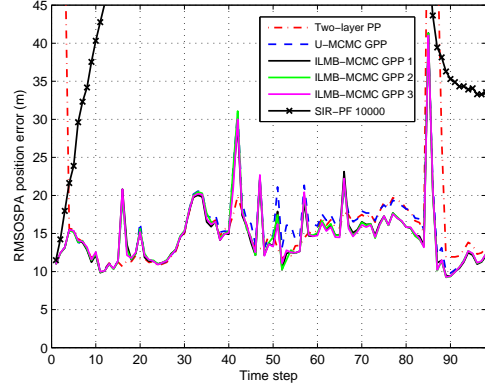
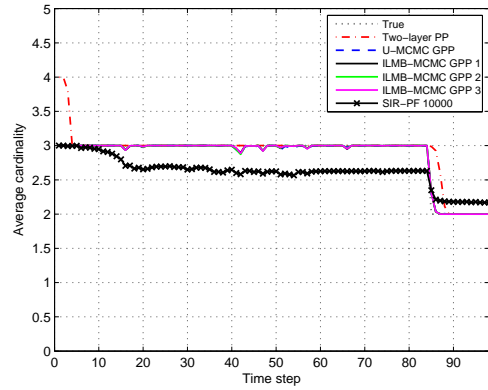


Figure 5: Scenario of the simulations. The target positions every ten time steps is represented by a circumference. The targets move from left to right. The sensor positions are represented by black crosses.



(a)



(b)

Figure 6: RMSOSPA position error (a) and average cardinality (b) against time for the scenario in Fig. 5. ILMB filters perform best especially after the targets have been in close proximity for some time. The two-layer PP PF has an inherent delay in removing tracks. SIR-PF with 10000 particles does not perform well.

of this is to clearly demonstrate the benefits of using LMB assumption and how it can improve filter performance. The root mean square OSPA (RMSOSPA) position errors [39] against time and average cardinality are shown in Figure 6. SIR-PF does not perform well even though it uses 10000 particles instead of 500. The two-layer PF in [4] has a bias to remove targets as it always requires several time steps. Therefore, error increases significantly when a target disappears. ILMB-GPP methods do not have this drawback and are able to provide a low error when targets disappear. In Figure 6 (a), there are several spikes in the error for ILMB-GPP algorithms. These spikes arise due to errors in cardinality estimation, as seen in Figure 6 (b). All the versions of GPP-ILMB provide an improvement over U-MCMC specially after time step 40 until around time step 90. The former corresponds to a time step in which the targets have been in close proximity for a while, see Figure 5. The GPP-ILMB implementations perform quite similarly. This implies that in this scenario one step of the LMB improvement sequence, described in Section III, makes a difference but further steps provide a negligible improvement.

Now, we analyse the effect of the number of particles on filter performance. We show the RMSOSPA error averaged

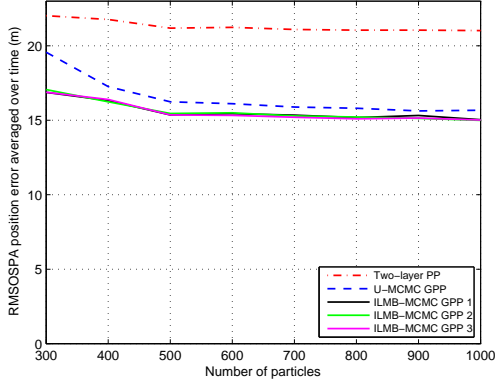


Figure 7: RMSOSPA position error averaged over time against the number of particles. ILMB performance is higher than the rest of the algorithms for different number of particles.

over time against the number of particles in Figure 7. Due to the bias in target state estimation of the two-layer PF, increasing the number of particles is not sufficient to lower the error. ILMB-MCMC algorithms have similar performance and outperform the U-MCMC. As expected, this improvement decreases as the particle number increases. For example, for 300 particles, the difference in error between U-MCMC and the best ILMB-MCMC is around 2.7 m while for 1000 particles it is 0.6 m. In addition, we want to recall that ILMB-MCMC and U-MCMC have basically the same error until time step 40 so the averaged error over time does not really show the differences between the filter performances when they really occur.

The computational complexity of ILMB-MCMC algorithms is slightly higher than for U-MCMC and the two-layer PF. For example, for 500 particles, the execution times in seconds of our Matlab implementation of the algorithms on an Intel Core i7 laptop are: Two-layer PP (11.4), U-MCMC GPP (10.29), ILMB-MCMC GPP 1 (12.1), 2 (12.7), 3 (12.0). Nevertheless, according to Figure 7, the error achieved by ILMB method using 500 particles is not achieved by U-MCMC even with 1000 particles. This implies that for a given objective error, we can lower the number of particles and the execution times if we use the MCMC algorithm developed in this paper. We also want to remark that the execution time of the SIR-PF with 10000 particles is 12.5s and has a significantly worse performance than the previous filters.

### B. Example with target births

We proceed to analyse the performance of the proposed algorithms in the scenario shown in Figure 8, which has target births, deaths and crossings though no targets are in close proximity for a long time. Therefore, as was demonstrated in the previous simulations, the improvement of the MCMC algorithm is expected to be negligible as there is no mixing of labels [7]. The objectives of this example are: show that the MCMC algorithm is only needed if there is mixing of labels and assess how the filters work if there are target births.

We use the same parameters as in the previous section. There are four possible locations of target births with birth

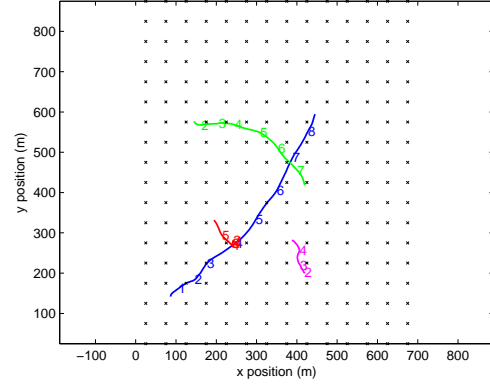


Figure 8: Scenario of the simulations with target births. Target positions at time step  $10k$  are marked by  $k$ . Targets are born at time steps (5, 10, 15, 20) and they die at time steps (90, 60, 80, 50). The sensor positions are represented by black crosses.

probability  $10^{-3}$  and densities  $\eta(\cdot; j) = \mathcal{N}(\cdot; m_j, 100I_4)$ , with  $m_1 = (85, 2, 140, 2)$ ,  $m_2 = (250, 0, 280, 0)$ ,  $m_3 = (145, 0, 575, 0)$  and  $m_4 = (420, 0, 200, 0)$  in international system units.

The proposed algorithms are implemented with 500 particles while the SIR-PF uses 10000 particles. We do not compare with the two-layer particle filter in [4] as it was designed for uniform birth models not for this kind of birth model. GPP has been implemented with and without U-MCMC and in this scenario both have similar performance. The RMSOSPA position error and average cardinality for the algorithms are shown in Figure 9. As before, SIR-PF has a much lower performance than the proposed algorithms. GPP and ILMB-GPP algorithms perform similarly. As indicated before, this is expected as targets are not in close proximity for a long time, as in Figure 5, so the effect of ILMB-MCMC is expected to be negligible as there is no mixing of labels [7]. GPP methods estimate the cardinality quite accurately at most time steps and provide low position errors.

In this case the execution times in seconds are: GPP (4.8), ILMB-MCMC GPP 1 (25.2), 2 (25.3), 3 (25.3) and SIR-PF (40). SIR-PF has a higher computational complexity because of the number of particles and possible labels it generates. The GPP method is able to sample labels more efficiently by the importance density (34). ILMB-MCMC algorithms have a high computational burden w.r.t. GPP because we perform the MCMC algorithm on all possible targets, which is inefficient. As we mention in Section V-C, in practice, we would apply clustering so that we only perform the MCMC steps for the targets that exhibit label mixing.

## VII. CONCLUSIONS

We have proposed the GPP-PF, which is a PF for general track-before-detect models under an LMB assumption. The GPP-PF can be applied on its own without the need of a label switching improvement algorithm, has a low computational burden and efficiently deals with target births and deaths.

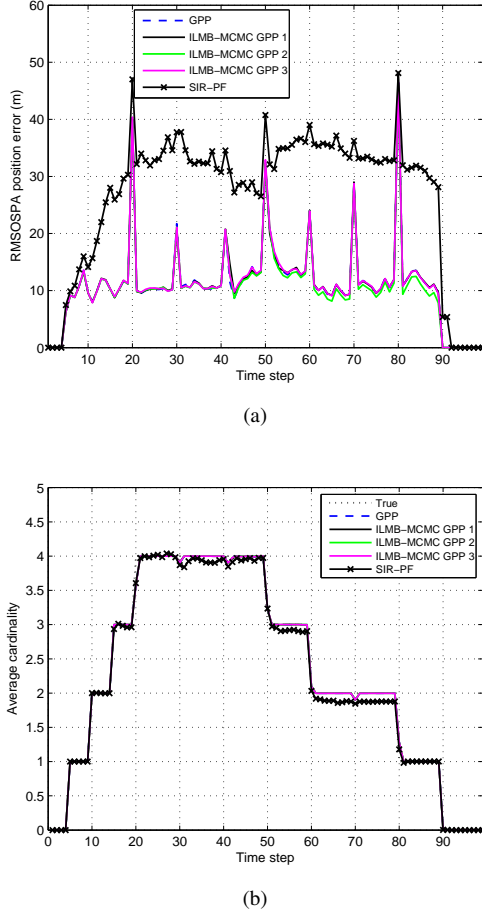


Figure 9: RMSOSPA position error (a) and average cardinality (b) against time for the scenario in Fig. 8. GPP methods with 500 particles outperform SIR-PF with 10000 particles.

We have also derived a label switching improvement algorithm. This kind of algorithm can be applied when we use a labelled posterior to approximate the unlabelled posterior. It is based on a sequence of PDFs that improves the LMB approximation from a member of the unlabelled RFS family of the posterior based on recursive KLD optimisations. The label switching improvement algorithm has been implemented and incorporated to the GPP-PF using an MCMC algorithm called ILMB-MCMC. The benefits of the ILMB-MCMC algorithm are expected to happen when targets get in close proximity for a long time and separate. As a result, if targets are not in close proximity for a sufficiently long time, we should use the GPP-PF without ILMB-MCMC to save computational resources. If targets get in close proximity for a sufficiently long time, we should use the GPP-PF along with ILMB-MCMC to improve tracking performance.

Future work should address how to perform clustering efficiently such that we only perform the ILMB-MCMC steps for the targets with labelling mixing. In addition, the algorithms should be adapted for Rao-Blackwellisation.

## APPENDIX A

In this appendix, we prove (6). We have that

$$\begin{aligned} D(\pi \parallel \nu) &= \int \pi(\mathbf{X}) \log \frac{\pi(\mathbf{X})}{\nu(\mathbf{X})} \delta \mathbf{X} \\ &= \sum_{t=0}^{\infty} \frac{1}{t!} \sum_{[l_1, \dots, l_t] \in \mathbb{L}^t} \int \pi(\{(x_1, l_1), \dots, (x_t, l_t)\}) \\ &\quad \times \log \frac{\pi(\{(x_1, l_1), \dots, (x_t, l_t)\})}{\nu(\{(x_1, l_1), \dots, (x_t, l_t)\})} dx_{1:t}. \end{aligned} \quad (62)$$

Using (3), we get

$$\begin{aligned} D(\pi \parallel \nu) &= \sum_{t=0}^{\infty} \frac{1}{t!} \sum_{l_{1:t} \in \mathbb{L}^t} \int \pi(x_{1:t}; l_{1:t}) P_{\pi}(\{l_1, \dots, l_t\}) \\ &\quad \times \log \frac{\pi(x_{1:t}; l_{1:t}) P_{\pi}(\{l_1, \dots, l_t\})}{\nu(x_{1:t}; l_{1:t}) P_{\nu}(\{l_1, \dots, l_t\})} dx_{1:t} \\ &= \sum_{t=0}^{\infty} \frac{1}{t!} \sum_{l_{1:t} \in \mathbb{L}^t} \left[ P_{\pi}(\{l_1, \dots, l_t\}) \log \frac{P_{\pi}(\{l_1, \dots, l_t\})}{P_{\nu}(\{l_1, \dots, l_t\})} \right. \\ &\quad \left. + P_{\pi}(\{l_1, \dots, l_t\}) \int \pi(x_{1:t}; l_{1:t}) \log \frac{\pi(x_{1:t}; l_{1:t})}{\nu(x_{1:t}; l_{1:t})} dx_{1:t} \right] \\ &= D(P_{\pi} \parallel P_{\nu}) + \sum_{t=0}^{\infty} \frac{1}{t!} \sum_{l_{1:t} \in \mathbb{L}^t} P_{\pi}(\{l_1, \dots, l_t\}) \\ &\quad \times D(\pi(\cdot; l_{1:t}) \parallel \nu(\cdot; l_{1:t})). \end{aligned} \quad (63)$$

As the last term is permutation invariant w.r.t.  $l_{1:t}$ , we get (6).

## APPENDIX B

In this appendix we prove Theorem 3. Due to the fact that the constraints are not coupled, we can first obtain the best PMF of the labels and then the PDF of the states given the labels. Then, we consider

$$\arg \min_{P_{\nu}} D(P_{\varphi} \parallel P_{\nu}) \quad (64)$$

subject to (7). Substituting (7) into (64), we can rewrite the optimisation problem in terms of the parameters  $p_1, \dots, p_{\kappa}$  subject to the constraint  $0 \leq p_i \leq 1$   $i \in \{1, \dots, \kappa\}$ . According to (7), for the sets in which  $i$  is included,  $P_{\nu}$  is proportional to  $p_i$  and otherwise it is proportional to  $1 - p_i$ , then, we have to minimise

$$\arg \min_{p_1, \dots, p_{\kappa}} \sum_{i=1}^{\kappa} f(p_i)$$

where

$$\begin{aligned} f(p_i) &= \text{ct} - \sum_{L \subseteq \mathbb{L}: i \in L} \log(p_i) P_{\varphi}(L) \\ &\quad + \sum_{L \subseteq \mathbb{L}: i \notin L} \log(1 - p_i) P_{\varphi}(L) \end{aligned} \quad (65)$$

for all  $i \in \mathbb{L}$  subject to  $0 \leq p_i \leq 1$ , where ct represents all the terms that do not depend on  $p_i$ . Function  $f(\cdot)$  is convex as it has the form of a KLD over a PMF of a discrete variable

with two states [40]. Calculating the derivative and setting it to zero, we get

$$p_i = \sum_{L \subseteq \mathbb{L}: i \in L} P_\varphi(L) \quad (66)$$

which completes the proof as  $0 \leq p_i \leq 1$ .

Second, for a given collection of PDFs  $\varphi(x_{1:t}; l_{1:t})$ ,  $\{l_1, \dots, l_t\} \subseteq \{1, \dots, \kappa\}$ , we obtain  $\nu(\cdot; 1) \dots \nu(\cdot; \kappa)$ , which meet (8), that minimise

$$\sum_{L \subseteq \mathbb{L}} P_\varphi(L) \int \varphi(x_{1:|L|}; \vec{L}) \log \frac{\varphi(x_{1:|L|}; \vec{L})}{\nu(x_{1:|L|}; \vec{L})} dx_{1:|L|}$$

We obtain the minimisation for  $\nu(\cdot; 1)$  although the result is general. Expanding the logarithm, we want to minimise the functional

$$\begin{aligned} A[\nu(\cdot; 1)] &= \text{ct} - \sum_{L \subseteq \mathbb{L}: 1 \in L} P_\varphi(L) \int \varphi_1(x_1; \vec{L}) \log \nu(x_1; 1) dx_1 \\ &\quad (67) \end{aligned}$$

where ct represents all the terms that do not depend on  $\nu(\cdot; 1)$  and  $\varphi_1(\cdot; \vec{L})$  is the marginal PDF of the first variable of  $\varphi(\cdot; \vec{L})$ . By KLD minimisation over vector spaces, this functional is minimised by [41]

$$\nu(x_1; 1) \propto \sum_{L \subseteq \mathbb{L}: 1 \in L} P_\varphi(L) \varphi_1(x_1; \vec{L}). \quad (68)$$

#### APPENDIX C

In this appendix, we prove Theorem 4. Given  $\varphi$ , its corresponding unlabelled density is [3]

$$\begin{aligned} \check{\varphi}(\{x_1, \dots, x_t\}) &= \sum_{l_{1:t} \in \mathbb{L}^t} \varphi(\{(x_1, l_1), \dots, (x_t, l_t)\}) \\ &= \sum_{l_{1:t} \in \mathbb{L}^t} P_\varphi(\{l_1, \dots, l_t\}) \varphi(x_{1:t}; l_{1:t}) \\ &= \sum_{\substack{\{l_1, \dots, l_t\} \subseteq \mathbb{L} \\ l_1 < \dots < l_t}} \sum_{p=1}^t P_\varphi(\{\Gamma_{p,t}(l_1, \dots, l_t)\}) \varphi(x_{1:t}; \Gamma_{p,t}(l_{1:t})) \\ &= \sum_{\substack{\{l_1, \dots, l_t\} \subseteq \mathbb{L} \\ l_1 < \dots < l_t}} P_\varphi(\{l_1, \dots, l_t\}) \check{\varphi}(\{x_1, \dots, x_t\}; l_{1:t}). \quad (69) \end{aligned}$$

Given  $\check{\nu}$ ,  $P_\varphi = P_\pi$ ,  $L$  and  $\varphi(\cdot; \vec{L}) \forall L' \neq L$ , we want to obtain  $\varphi(\cdot; \vec{L})$  that minimises  $D(\check{\varphi} \parallel \check{\nu})$  subject to  $\varphi \in [\pi]$ . Due to the way the sequence is constructed, constraint  $\varphi \in [\pi]$  can be written as

$$\check{\varphi}(\{x_1, \dots, x_t\}; \vec{L}) = \check{\pi}(\{x_1, \dots, x_t\}; \vec{L}). \quad (70)$$

In the KLD, there is only one term that depends on  $\varphi(\cdot; \vec{L})$  so we only need to minimise the functional

$$A[\varphi(\cdot; \vec{L})] = \int \varphi(x_{1:t}; \vec{L}) \log \frac{\varphi(x_{1:t}; \vec{L})}{\nu(x_{1:t}; \vec{L})} dx_{1:t} \quad (71)$$

subject to constraint (70). This minimisation was solved in [31, Appendix C] and its result is provided in Theorem 4. A quite similar proof for a two-target case with Gaussian PDFs is found in [42].

#### APPENDIX D

In this appendix we prove that the target PDF is invariant w.r.t. the transition rule of the MCMC algorithm in Section V-B. Here, we denote the transition PDF  $\pi(\cdot)$  and the transition density to go from  $x_{1:t}$  to  $y_{1:t}$  as  $A(x_{1:t}, y_{1:t})$  and the number of targets is  $t$ . This is proved by the detailed balance condition [10]

$$\pi(x_{1:t}) A(x_{1:t}, y_{1:t}) = \pi(y_{1:t}) A(y_{1:t}, x_{1:t}) \quad (72)$$

where  $\pi(\cdot)$  denotes a general objective PDF, e.g., in Section V-B, this corresponds to  $\varphi^n(x_{1:|L|} | a_{1:|L|}; \vec{L})$  as the MCMC moves are only proposed in variable  $x_{1:|L|}$ .

According to Section V-B, we can write the transition density  $A(x_{1:t}, y_{1:t}, \cdot)$  as

$$\begin{aligned} A(x_{1:t}, y_{1:t}, \cdot) &= \sum_{p=1}^t \frac{q(\Gamma_{p,t}(y_{1:t}) | x_{1:t})}{t!} r(x_{1:t}, y_{1:t}) \\ &\quad + \left(1 - \int \sum_{p=1}^t \frac{q(\Gamma_{p,t}(y_{1:t}) | x_{1:t})}{t!} r(x_{1:t}, y_{1:t}) dy_{1:t}\right) \\ &\quad \times \frac{1}{\sum_{p=1}^t \pi(\Gamma_{p,t}(x_{1:t}))} \sum_{p=1}^t \pi(y_{1:t}) \delta(y_{1:t} - \Gamma_{p,t}(x_{1:t})) \quad (73) \end{aligned}$$

where the acceptance probability of  $y_{1:t} \neq \Gamma_{p,t}(x_{1:t})$  is

$$r(x_{1:t}, y_{1:t}) = \frac{\pi(y_{1:t})}{\sum_{p=1}^t [\pi(\Gamma_{p,t}(y_{1:t})) + \pi(\Gamma_{p,t}(x_{1:t}))]}. \quad (74)$$

Then,

$$\begin{aligned} \pi(x_{1:t}) A(x_{1:t}, y_{1:t}) &= \sum_{p=1}^t \frac{q(\Gamma_{p,t}(y_{1:t}) | x_{1:t})}{t!} \\ &\quad \times \frac{\pi(y_{1:t}) \pi(x_{1:t})}{\sum_{p=1}^t [\pi(\Gamma_{p,t}(y_{1:t})) + \pi(\Gamma_{p,t}(x_{1:t}))]} \\ &\quad + \left(1 - \int \sum_{p=1}^t \frac{q(\Gamma_{p,t}(y_{1:t}) | x_{1:t})}{t!} r(x_{1:t}, y_{1:t}) dy_{1:t}\right) \\ &\quad \times \frac{\pi(y_{1:t}) \pi(x_{1:t})}{\sum_{p=1}^t \pi(\Gamma_{p,t}(x_{1:t}))} \sum_{p=1}^t \delta(y_{1:t} - \Gamma_{p,t}(x_{1:t})). \quad (75) \end{aligned}$$

As  $q(y_{1:t} | x_{1:t}) = \prod_{j=1}^t q'(y_j | x_j)$ , if  $q'(\cdot | \cdot)$  is symmetric, we get (72), which completes the proof.

## REFERENCES

- [1] R. P. S. Mahler, *Advances in Statistical Multisource-Multitarget Information Fusion*. Artech House, 2014.
- [2] —, “Multitarget Bayes filtering via first-order multitarget moments,” *IEEE Transactions on Aerospace and Electronic Systems*, vol. 39, no. 4, pp. 1152–1178, Oct. 2003.
- [3] B. T. Vo and B. N. Vo, “Labeled random finite sets and multi-object conjugate priors,” *IEEE Transactions on Signal Processing*, vol. 61, no. 13, pp. 3460–3475, July 2013.
- [4] A. F. García-Fernández, J. Grajal, and M. R. Morelande, “Two-layer particle filter for multiple target detection and tracking,” *IEEE Transactions on Aerospace and Electronic Systems*, vol. 49, no. 3, pp. 1569–1588, July 2013.
- [5] A. F. García-Fernández and M. R. Morelande, “Explicit filtering equations for labelled random finite sets,” in *Fourth International Conference On Control Automation and Information Sciences*, 2015, pp. 349–354.
- [6] L. Svensson, D. Svensson, M. Guerriero, and P. Willett, “Set JPDA filter for multitarget tracking,” *IEEE Transactions on Signal Processing*, vol. 59, no. 10, pp. 4677–4691, Oct. 2011.
- [7] Y. Boers, E. Sviestins, and H. Driessen, “Mixed labelling in multitarget particle filtering,” *IEEE Transactions on Aerospace and Electronic Systems*, vol. 46, no. 2, pp. 792–802, April 2010.
- [8] J. L. Williams, “An efficient, variational approximation of the best fitting multi-Bernoulli filter,” *IEEE Transactions on Signal Processing*, vol. 63, no. 1, pp. 258–273, Jan. 2015.
- [9] B. Ristic, S. Arulampalam, and N. Gordon, *Beyond the Kalman Filter: Particle Filters for Tracking Applications*. Artech House, 2004.
- [10] J. S. Liu, *Monte Carlo Strategies in Scientific Computing*. Springer, 2001.
- [11] R. Mahler, “PHD filters of higher order in target number,” *IEEE Transactions on Aerospace and Electronic Systems*, vol. 43, no. 4, pp. 1523–1543, October 2007.
- [12] S. Blackman and R. Popoli, *Design and Analysis of Modern Tracking Systems*. Artech House, 1999.
- [13] S. Reuter, B.-T. Vo, B.-N. Vo, and K. Dietmayer, “The labeled multi-Bernoulli filter,” *IEEE Transactions on Signal Processing*, vol. 62, no. 12, pp. 3246–3260, June 2014.
- [14] B.-N. Vo, B.-T. Vo, and D. Phung, “Labeled random finite sets and the Bayes multi-target tracking filter,” *IEEE Transactions on Signal Processing*, vol. 62, no. 24, pp. 6554–6567, Dec. 2014.
- [15] J. Vermaak, S. J. Godsill, and P. Perez, “Monte Carlo filtering for multi target tracking and data association,” *IEEE Transactions on Aerospace and Electronic Systems*, vol. 41, no. 1, pp. 309–332, Jan. 2005.
- [16] S. Särkkä, A. Vehtari, and J. Lampinen, “Rao-Blackwellized particle filter for multiple target tracking,” *Information Fusion*, vol. 8, no. 1, pp. 2–15, Jan. 2007.
- [17] S. Nannuru, M. Coates, and R. Mahler, “Computationally-tractable approximate PHD and CPHD filters for superpositional sensors,” *IEEE Journal of Selected Topics in Signal Processing*, vol. 7, no. 3, pp. 410–420, June 2013.
- [18] F. Papi and D. Y. Kim, “A particle multi-target tracker for superpositional measurements using labeled random finite sets,” *IEEE Transactions on Signal Processing*, vol. 63, no. 16, pp. 4348–4358, Aug. 2015.
- [19] B.-N. Vo, B.-T. Vo, N.-T. Pham, and D. Suter, “Joint detection and estimation of multiple objects from image observations,” *IEEE Transactions on Signal Processing*, vol. 58, no. 10, pp. 5129–5141, Oct. 2010.
- [20] C. Kreucher, K. Kastella, and A. O. Hero III, “Multitarget tracking using the joint multitarget probability density,” *IEEE Transactions on Aerospace and Electronic Systems*, vol. 41, no. 4, pp. 1396–1414, Oct. 2005.
- [21] M. R. Morelande, C. M. Kreucher, and K. Kastella, “A Bayesian approach to multiple target detection and tracking,” *IEEE Transactions on Signal Processing*, vol. 55, no. 5, pp. 1589–1604, May 2007.
- [22] M. Fallon and S. Godsill, “Acoustic source localization and tracking of a time-varying number of speakers,” *IEEE Transactions on Audio, Speech, and Language Processing*, vol. 20, no. 4, pp. 1409–1415, May 2012.
- [23] S. Davey, M. Wieneke, and H. Vu, “Histogram-PMHT unfettered,” *IEEE Journal of Selected Topics in Signal Processing*, vol. 7, no. 3, pp. 435–447, June 2013.
- [24] F. Septier, S. K. Pang, A. Carmi, and S. Godsill, “On MCMC-based particle methods for Bayesian filtering: Application to multitarget tracking,” in *3rd IEEE International Workshop on Computational Advances in Multi-Sensor Adaptive Processing*, Dec 2009, pp. 360–363.
- [25] P. Del Moral and L. Miclo, “Branching and interacting particle systems approximations of Feynman-Kac formulae with applications to non-linear filtering,” in *Séminaire de Probabilités XXXIV*. Springer, 2000, vol. 1729, pp. 1–145.
- [26] M. Orton and W. Fitzgerald, “A Bayesian approach to tracking multiple targets using sensor arrays and particle filters,” *IEEE Transactions on Signal Processing*, vol. 50, no. 2, pp. 216–223, Feb. 2002.
- [27] W. Yi, M. R. Morelande, L. Kong, and J. Yang, “A computationally efficient particle filter for multitarget tracking using an independence approximation,” *IEEE Transactions on Signal Processing*, vol. 61, no. 4, pp. 843–856, 2013.
- [28] L. Úbeda-Medina, A. F. García-Fernández, and J. Grajal, “Generalizations of the auxiliary particle filter for multiple target tracking,” in *17th International Conference on Information Fusion*, 2014.
- [29] Y. Boers and J. N. Driessen, “Multitarget particle filter track before detect application,” *IEE Proceedings Radar, Sonar and Navigation*, vol. 151, no. 6, pp. 351–357, Dec. 2004.
- [30] A. F. García-Fernández, M. R. Morelande, and J. Grajal, “Bayesian sequential track formation,” *IEEE Transactions on Signal Processing*, vol. 62, no. 24, pp. 6366–6379, Dec. 2014.
- [31] A. F. García-Fernández, B.-N. Vo, and B.-T. Vo, “MCMC-based posterior independence approximation for RFS multitarget particle filters,” in *17th International Conference on Information Fusion*, 2014.
- [32] A. F. García-Fernández and J. Grajal, “Multitarget tracking using the joint multitrack probability density,” in *12th International Conference on Information Fusion*, July 2009, pp. 595–602.
- [33] B. Kolman, R. C. Busby, and S. C. Ross, *Discrete Mathematical Structures*. Pearson, 2001.
- [34] M. K. Pitt and N. Shephard, “Filtering via simulation: Auxiliary particle filters,” *Journal of the American Statistical Association*, vol. 94, no. 446, pp. 590–599, Jun. 1999.
- [35] X. Sheng and Y.-H. Hu, “Maximum likelihood multiple-source localization using acoustic energy measurements with wireless sensor networks,” *IEEE Transactions on Signal Processing*, vol. 53, no. 1, pp. 44–53, Jan. 2005.
- [36] M. Arulampalam, S. Maskell, N. Gordon, and T. Clapp, “A tutorial on particle filters for online nonlinear/non-Gaussian Bayesian tracking,” *IEEE Transactions on Signal Processing*, vol. 50, no. 2, pp. 174–188, Feb. 2002.
- [37] D. Schuhmacher, B.-T. Vo, and B.-N. Vo, “A consistent metric for performance evaluation of multi-object filters,” *IEEE Transactions on Signal Processing*, vol. 56, no. 8, pp. 3447–3457, Aug. 2008.
- [38] M. Guerriero, L. Svensson, D. Svensson, and P. Willett, “Shooting two birds with two bullets: How to find minimum mean OSPA estimates,” in *13th Conference on Information Fusion*, July 2010, pp. 1–8.
- [39] A. S. Rahmathullah, A. F. García-Fernández, and L. Svensson, “Generalized optimal sub-pattern assignment metric,” 2016. [Online]. Available: <http://arxiv.org/abs/1601.05585>
- [40] S. Boyd and L. Vandenberghe, *Convex Optimization*. Cambridge University Press, 2004.
- [41] C. M. Bishop, *Pattern Recognition and Machine Learning*. Springer Science + Business Media, 2006.
- [42] L. Svensson, D. Svensson, and M. Guerriero, “Set JPDA filter for multiple target tracking,” Chalmers University of Technology, Tech. Rep. R012/2010, 2010.